Check for updates

Journal of Science and Engineering Papers
eISSN- 3094-1182 | pISSN- 3079-8175
DOI- 10.62275/josep.24.1000001

REVIEW ARTICLE OPEN ACCESS

Multi-Physical Aging and Degradation of Concrete Containments and Biological Shields in Nuclear Power Plants: A Critical Review of Radiation-Induced Damage, Shielding Physics, and Predictive Management Frameworks

Dipayan Sikder[1*] | Md. Maidul Islam[2] | Md. Shojib Mia[2] | Quazi Md. Zobaer Shah[1] | Shahpara Sheikh Dola[1] | Prodip Kumar Sarkar[3] | Mohammad Toufiqur Rahman[3]

[1]Nuclear Safety Division, Bangladesh Atomic Energy Regulatory Authority, Dhaka, Bangladesh
[2]Nuclear Safeguards Division, Bangladesh Atomic Energy Regulatory Authority, Dhaka, Bangladesh
[3]Department of Civil Engineering, Khulna University of Engineering and Technology

Correspondence: Dipayan Sikder (sikder.dipayan@gmail.com)

Received: 02 September 2026 | **Revised:** 15 September 2026 | **Accepted:** 16 September 2026 | **Available Online:** 17 November 2026

ABSTRACT

In nuclear power plants (NPPs), reinforced concrete structures play a vital role as safety-related assets, serving as a structural support, leak-tight enclosure and biological radiation shielding. These structures are physically and chemically degraded in extended operating lifespans (60 to 80+ years) in strong thermal, neutron and gamma radiation fields. This review aims at presenting a multi-physical rigorous synthesis of concrete aging mechanisms. The main effects of fast neutrons are atomic displacement, crystalline disorder (metamictization) and Radiation-Induced Volumetric Expansion (RIVE) of mineral aggregates, while the main effects of gamma rays are pore-water radiolysis, C-S-H degradation and matrix drying shrinkage. This causes localized tensile stresses and extensive microcracking at the Interfacial Transition Zone (ITZ). At the macrostructural level, the paper summarizes the degradation analysis of reinforced concrete panels under multi-axial loading using the Modified Compression Field Theory (MCFT) that shows a capacity loss of up to 62% at high fast neutron fluences (2.0×10^{21} n/cm^2) for heavily reinforced panels ($\rho > 1.88\%$) and a clear failure mode transition from ductile steel yielding to brittle concrete crushing. Moreover, mitigation strategies such as advanced shielding aggregates (magnetite) and nano-engineered hybrids (1.5% nano-alumina and 0.1% carbon nanotubes) are assessed. This study presens a risk-informed, probabilistic ageing management program (AMP) that combines advanced non-destructive testing (NDT) to ensure nuclear safety around the world, reconciling laboratory models with the empirical field data from decommissioned biological shields (JPDR) and CANDU containments.

Keywords: *Radiation-Induced Volumetric Expansion (RIVE), Heavyweight Shielding Concrete, Metamictization, Modified Compression Field Theory (MCFT), Aging Management Program (AMP).*

1 | Introduction

The world's nuclear energy market is going through a historic transformation. Economic incentives and carbon-neutral targets have led utilities to reach for license renewals and long-term operation (LTO) authorizations to extend plant life to 60, 80, or even 100 years originally designed and licensed for 30 to 40 years life [1]. In addition, modern decommissioning plans often call for reactors to be placed in a 'safe store' or 'static state' for a period of up to 100 years, requiring continuous containment integrity, leak-tightness and radiation shielding to be maintained. Safety-related civil structures such as the primary reactor containment building, internal biological shield walls, auxiliary structures and spent fuel pools are passive, massive and virtually irreplaceable, in contrast to mechanical and electrical components which can be replaced on a routine basis [1]. The life extension physical and regulatory feasibility is thus determined by their durability and functional capacity.

The regulatory regime in the United States for the License Renewal Rule (10 CFR Part 54) and Maintenance Rule (10 CFR Part 50.65) is under the control of the Nuclear Regulatory Commis-

This is an open access article under the terms of the Creative Commons Attribution-ShareAlike 4.0 International license (CC BY-SA 4.0), which permits usage, distribution, and replication in any format as long as the original work is correctly attributed and published here first, and the original work is properly cited.

© 2027 The Author(s). Journal of Science and Engineering Papers

sion (USNRC) [2]. The license renewal reviews are limited to passive, long-lived structures and components. The USNRC created the Generic Aging Lessons Learned (GALL) Report to provide a technical foundation for these assessments and identifies areas in which aging management programs (AMPs) need to be supplemented [2]. The GALL report requires detailed, time-limited aging analyses (TLAAs) for civil structures to be performed to show that the required safety margins are not degraded over the extended operating life by environment and synergistic degradation factors [2].

The main civil safety related asset is the concrete containment building which forms the last physical barrier to the uncontrolled release of radioactive fission products during normal operation and design basis accident (DBA) including a loss of coolant accident (LOCA) [1, 3]. The primary containment is usually a large diameter concrete shell, either conventional reinforced concrete (RCC) with wall thicknesses of about 1.4 m, hemispherical dome with 1.1 m, or thick basemat concrete foundations, or post-tensioned concrete (PTC) systems with unbonded tendon systems. An internal carbon steel liner plate between 6.35mm and 12.7mm thick ensures leak-tightness. The biological shield wall is a secondary critical system that is located near the reactor core, and is used to reduce high intensity neutron and gamma radiation to the personnel and internal components [3, 4]. In these systems, as they mature, they are subjected to harsh thermal and radiation conditions, which require a paradigm shift from prescriptive inspection methods based on intervals to advanced, predictive and multi-physical aging management [4].

1.1 | Review Methodology

The scope of this review was designed in a multi-tier literature search strategy to ensure the critical synthesis was systematic, transparent and reproducible. Out of 145 initial literatures, 22 core landmark studies were chosen for in-depth comparative synthesis, which attends to the atomic displacement phenomena and the macro-structural capacity loss and risk-informed structural health prognosis.

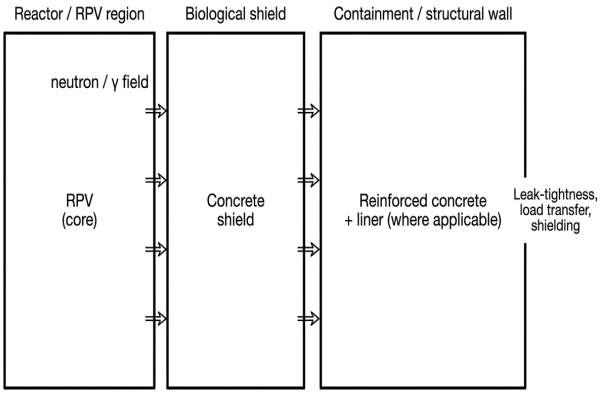


Figure 1 | The simplified orientation schematic is shown with the reactor region, biological shield, and reinforced-concrete containment/structural wall. This is a conceptual figure and not plant specific.

Inclusion criteria focused on:

(i) Established basic physical models of the microstructural radiation damage in aggregates and cement paste;

(ii) Empirical field data obtained from real decommissioned NPP civil assets (JPDR, Gentilly-1 and Gentilly-2);

(iii) Validated multi-axial structural panel formulations using Modified Compression Field Theory (MCFT) and Membrane-2000; and

(iv) Standardized regulatory oversight and ageing management systems (USNRC GALL and IAEA Safety Standards).

2 | Micrstructural and Chemical Mechanisms of Radiation-Induced Concrete Degradation

Structural concrete exposed to radiation fields undergoes complex physical, chemical and mineralogical changes. Concrete is a heterogeneous composite which is composed of coarse/fine mineral aggregates and hardened cement paste (HCP). Practical guidelines for the historical consensus were set forth by the seminal review of Hilsdorf et al. [5] and Kaplan [6] which indicated that concrete up to fast neutron fluences of 1.0×10^{19} n/cm^2 (E > 0.1 MeV) and integrated gamma doses of 1.0×10^8 Gy (or 10^{10} rads) experienced no significant degradation. But, based on the experience of the last few years in concrete production and the most up-to-date laboratory testing, it has been found that these limits are very sensitive to the concrete mixture, moisture condition, temperature and environment boundaries, so that new research programs are being undertaken in Japan, the USA, and Europe to redefine the limits of soundness [7].

2.1 | Fast Neutron Radiation and Radiation-Induced Volumetric Expansion (RIVE)

The fast neutrons are mainly interacting with the mineral structure of the concrete aggregates which are crystalline. Fast neutrons knock atoms out of their stable lattice sites through high-energy elastic collisions, forming interstitial-vacancy defects (Frenkel pairs). The displacement of atoms, which is called as metamictization, progressively destroys the long range crystallographic order of minerals, leading to their isotropic, disordered and amorphous state [8]. The main effect of metamictization is the Radiation-Induced Volumetric Expansion (RIVE) [8]. The aggregate mineralogy is the most significant factor affecting the extent and rate of RIVE [7, 8] Siliceous, felsic and silica based aggregates with minerals such as α-quartz (quartzites, flint, and

felsic sandstones) are particularly susceptible. If the fast neutron fluence is high, >1.0 × 10^{20} n/cm^2, crystalline quartz will swell as much as 15% to 20% volumetrically [8]. Carbonate based aggregates (limestones, for example) show a moderate swelling, while the swelling of the serpentine aggregates (magnesium silicate hydrate) is low, with only 0.1% swelling at a fluence of 5.0 × 10^{19} n/cm^2 [7].

The model equation for the kinetics of RIVE is derived based on an exponential growth model describing the expansion transition from crystalline to the fully amorphous state:

$$\frac{\Delta V}{V} = A \cdot [1 - e^{-B\phi}] \quad (1)$$

where ΔV / V is the fractional volumetric change induced by the radiation, Φ is the integrated fast neutron fluence (n/cm^2), and A and B are the empirical material constants which control the maximum volumetric expansion limit and the aggregate susceptibility rate respectively [8, 9]. Figure 2 represents the Eq (1) where curves are illustrative and are not experimental data; they demonstrate why A and B must be calibrated for the material and irradiation condition. Table 1 shows representative empirical RIVE kinetic parameters for major aggregate mineralogies.

2.2 | The Formation of Gamma Radiation, Radiolysis and Pore-Water Dehydration

However, gamma photons are not massive enough to cause material damage from direct atomic displacement in mineral lattices like fast neutrons are. Rather, gamma radiation leaves significant electronic ionization, free radicals and nuclear heating [10]. The main degradation mechanism for gamma damage in structural concrete is the radiolysis of the pore water [11]. Free, capillary and chemically bound water molecules in the HCP are dissociated in the presence of photons with high energy into hydrogen (H_2), oxygen (O_2) and hydrogen peroxide (H_2O_2) gases [11]. This radiolysis will effectively dehydrate the cement paste

Table 1 | Representative empirical RIVE kinetic parameters for major aggregate mineralogies [7-9].

Aggregate Mineralogy Class	Asymptotic Limit A (% Vol Expansion)	Susceptibility Factor B (10^{-20} cm^2/n)	RIVE Susceptibility
Quartzite / Felsic Aggregates (α-Quartz)	18.0 %	1.20 × 10^{-20}	Extreme
Calcareous / Limestone (Calcite)	3.0 %	0.80 × 10^{-20}	Moderate
Serpentine Aggregates (Mg-Silicate)	0.10 %	0.50 × 10^{-20}	Highly Stable

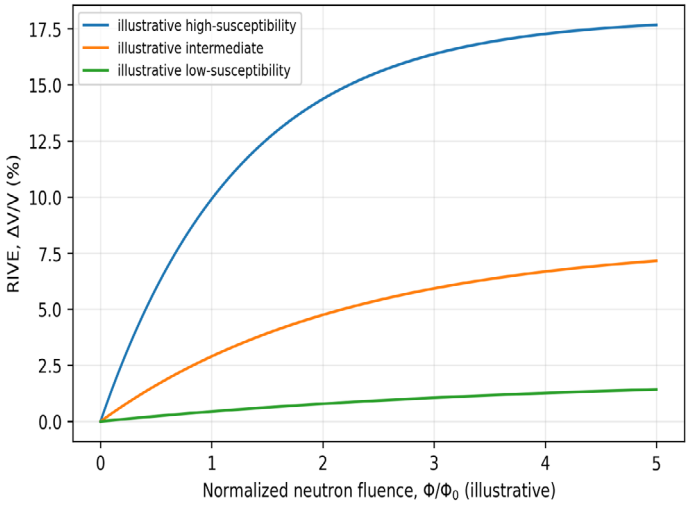


Figure 2 | Illustrative RIVE kinetics generated from the generic form of Eq. (1).

matrix, causing a change in hydration products, e.g. C-S-H, and microstructural drying shrinkage [11]. In addition, the radiolysis caused by the gamma rays and heating of the concrete will accelerate the carbonation process. This reaction uses up calcium hydroxide ($Ca(OH)_2$), reducing the pH of the cement pore solution from above 12.5 to below 9, which depassivates the embedded mild steel reinforcement and starts corrosion to increase in pace [7].

2.3 | Synergistic Volume Mismatch and Interfacial Degradation

Neutron and gamma radiation are generated together in a real world operating reactor primary shield, which results in a highly deleterious synergistic degradation. Fast neutrons cause the volume of mineral aggregates to expand and swell; gamma radiation and nuclear heating cause the cement paste surrounding the mineral aggregates to shrink and contract. This simultaneous and opposing volumetric movement causes an internal volume mismatch and strain incompatibility between the aggregate and the cement paste at the interface [9]. The Interfacial Transition Zone (ITZ) is a region of high localized tensile stresses. When these stresses become greater than the tensile strength of the mortar, a large number of microcracks develop and grow around the aggregate boundaries, and the load transfer capacity and structural integrity of the mortar are compromised [9]. It has been reported that if concrete is submerged in water, the gamma induced shrinkage can be reduced by replenishing capillary water but the basic incompatibility between the matrix shrinkage and aggregate swelling cannot be reduced [9].

The Classical Thresholds and Modern Multi-Axial Degradation Models are reconcilable as follows:

Historical reviews (Hilsdorf et al [5] and Kaplan [6]) defined no-damage threshold limits of fast neutron fluence < 1.0 × 10^{19}

n/cm² and gamma dose < 1.0 × 10^8 Gy, mainly based on unconfined uniaxial laboratory testing of individual specimens. Based on modern operational evaluations (Kambayashi et al. [9] and Maruyama et al [7]), under real world multi-axial stress states and restraint boundary conditions, localized ITZ microcracking and ITZ tensile strength degradation occurs at fluences around 2.0 × 10^{19} n/cm² (Degradation Level D1) in massive structural containments. Multi-axial shear capacity and tensile resistance is immediately reduced at this level, while the unconfined compressive strength does not seem to be affected, and perhaps increases due to the localized matrix-aggregate boundary debonding.

3 | Physics of Concrete Radiation Shielding and Advanced Materials Engineering

Radiation biological shields are designed to reduce both fast neutrons and high-energy gamma-ray photons [6]. The standard weight concrete (density ~2.3 g/cm³) used traditionally, is often restricted by structural thickness requirements. Heavyweight or dense type of shielding concretes are used to increase the shielding efficiency and to decrease the thickness of wall, which include heavy natural aggregates such as barite, magnetite, limonite and ilmenite, or artificial metallic additives [6].

3.1 | The Physics of Neutron Scattering and Gamma Absorption

The physics of radiation shielding determines two different mechanisms for the attenuation of neutron and photon radiation [10]. The absorption and scattering of high energy photons is dominated by interactions with the electron shells of heavy elements and the linear attenuation coefficient μ is linearly related to the density (ρ) of the material through which the photons pass (concrete):

$$I_{(x)} = I_0 \cdot e^{-\mu \cdot x} \quad (2)$$

where $I_{(x)}$ represents the radiation intensity at depth x and I0 is the incident intensity [10]. Figure 3 interprets Eq (2) where the curves are mathematical examples, not plant-specific shielding calculations.

In order to assess the shielding performance, engineers use the Half-Value Layer (HVL) thickness, which is the depth of the concrete needed to reduce incident gamma-ray intensity by half:

$$HVL = \frac{ln(2)}{\mu} \quad (3)$$

The addition of heavyweight aggregates like magnetite (Fe_3O_4, density 3.53 g/cm³) and barite ($BaSO_4$, density 3.35 g/cm³) has a tremendous effect on the concrete density, maximizing μ and minimizing HVL [6, 10].

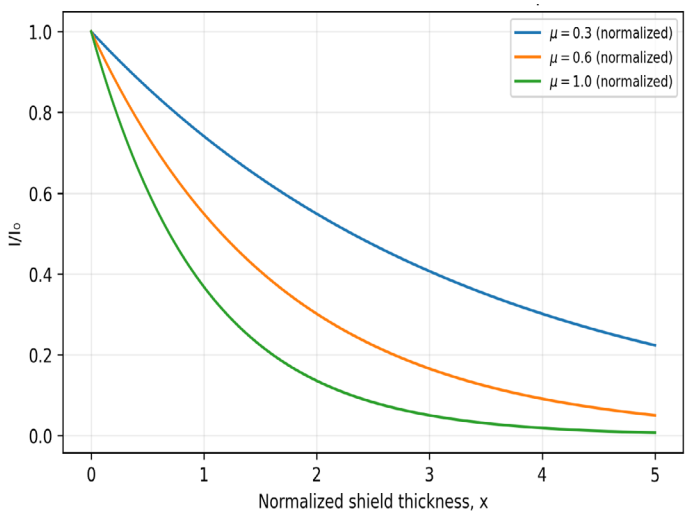


Figure 3 | Illustrative normalized photon attenuation using Eq. (2).

Neutron shielding is, however, a multi stage process that involves slowing down (thermalization) and then absorption [10]. The high-energy fast neutrons are thermalized through elastic scattering with light nuclei, and most prominently, with hydrogen. The Hydrogen in the pore water and crystallization water of concrete aggregates (e.g. serpentine and limonite) has an unusually large neutron scattering cross-section of 99.0 barns (1 barn = 10-28 m²) [6, 10]. After slowing neutrons to thermal energies (energy < 0.5 eV) they are captured by elements which have large thermal neutron capture cross-sections. The best absorption additive is boron-10, which has a huge capture cross-section of 755.0 barns [10]. Neutrons that are captured by boron emit very low-energy, non-penetrating alpha and gamma rays, and those captured by iron or calcium emit highly penetrating secondary gammas (E ~ 7 MeV), making it difficult to design shielding [10, 12]. Table 2 consists of physical and nuclear shielding parameters of major concrete constituents.

Table 2 | Physical and nuclear shielding parameters of major concrete constituents [6, 10, 12].

Shielding Constituent	Bulk Density Source	Scattering Cross-Section (barns)	Absorption Cross-Section (barns)
Hydrogen (H)	Capillary/ Crystalline Water	99.0	0.3
Oxygen (O)	Silicates/ Carbonates	4.2	0.0
Calcium (Ca)	Hydrated Cement Paste	3.0	0.4
Iron (Fe)	Magnetite / Hematite	11.0	2.5
Boron-10 (^{10}B)	Borated Additives	4.0	755.0

3.2 | Advanced Materials Engineering: SCMs, Fibers and Nano-hybrids

The contemporary civil engineering has presented enhanced mixtures to alleviate the degradation caused by radiations [13]. Supplementary cementitious materials (SCM), such as fly ash, ground granulated blast furnace slag (GGBFS), silica fume and metakaolin are also added as partial cement replacements [13]. The pozzolanic reactions of the SCSs break down calcium hydroxide to produce more calcium silicate hydrate (C-S-H) gel, which refines the pore structure and decreases water permeability [13]. Up to 5% replacement of cement with silica fume optimizes compaction and enhances durability in extreme environments [13]. Moreover, fiber reinforcement, which is the use of high-strength steel fibers, glass fibers or basalt fibers, offers essential post-cracking tensile capacity. Fibers fill microcracks at the boundaries of aggregates and mortars and stop crack propagation, maintaining structural ductility during thermal and radiation stresses [13].

Nano-engineered concrete is the future of radiation shielding design. The nano-additives can be incorporated in the process of controlling and optimizing physio-mechanical and chemical properties on the molecular level [14]. The combination of 1.5% nano-alumina (NA) and 0.1% carbon nanotubes (CNTs) by weight of cement in the form of a hybrid formulation leads to the maximum performance with considerable increases in compressive and flexural strength retention, cement paste microstructure densification to reduce water absorption, and gamma and neutron shielding performance at high thermal and radiation levels [14].

4 | Empiricism vs. Reality: Decommissioning Core Investigations and Non-Destructive Testing

Although laboratory research gives important baseline parameters, actual NPP constructions are exposed to low dose rate, long-term exposures throughout decades. To compare laboratory results and field performance, it is necessary to extract and test concrete core samples of decommissioned plants, and to conduct a high level of non-destructive testing (NDT) [7].

4.1 | The JPDR Biological Shield Investigation and Microstructural Anomalies

The largest field study of irradiated concrete was done on the biological shield of the Japan Power Demonstration Reactor (JPDR) when decommissioning it [15]. The JPDR had a 25-year service life, and its biological shield was subjected to the highest allowable estimated neutron fluence of fast neutrons of 1.11×10^{18} n/cm^2 and a cumulative gamma dose of 4.77×10^8 Gy at the reactor core level [15]. Shield extracted cores were thoroughly tested, both mechanically and chemically and petrographically and compared with non-irradiated mock-up concrete that was cured under the same thermal conditions [15].

Remarkably, no mechanical strength deterioration was obtained in unconfined compressive tests [15]. The compressive strength of the biological shield cores was between 29.4 and 53.0 Mpa (mean 44.0 Mpa) which was around 20 percent better than the original design mixing strength of 35 Mpa [15]. Static elasticity modulus and Poisson ratio also were steady, which points to the great macrostructural stability. An inner lining plate of 13 mm steel was used to prevent loss of moisture and enhance further hydration and strength development of the concrete [15]. Nonetheless, the scanning electron microscopy (SEM) of mortar samples of the high-radiation regions showed an unusual microstructural phenomenon: the colossal crystal formation of needle-like ettringite. During normal cement hydration, the initial ettringite is dissolved and transformed to monosulfate. The unusual stability and growth of large ettringite crystals in the high-radiation, high-temperature reactor-side zone means that radiation exposure changes microstructural crystallization kinetics, by processes that are still essentially unexplained within conventional hydration models.

4.2 | CANDU Plant Case Studies: Gentilly-1 and Gentilly-2 Containments

Atomic Energy of Canada Limited (AECL) CANDU plants experience in the field points out the criticality of aging management [16]. The Hydro-Québec headquarters built a four-level AMP in the Gentilly-2 NPP concrete containment building [16]. Alkali-Aggregate Reaction (AAR), a chemical reaction that forms an expansive silica gel in the event of moisture, was identified as the main threat and leads to severe macro-cracking [16]. To control this, structural engineers came up with non-linear finite element model that was calibrated on CSA Standard N287.7-08. Integration of this numerical tool enabled the utility to model swelling due to the AAR and forecast the risk of splitting (delamination) of concrete in the post-tensioning planes, which is essential in supporting remedial and mitigation measures when the license is renewed [16].

Likewise, the visual inspections of the decommissioned Gentilly-1 containment structure showed serious cracking and spalling of the secondary concrete shielding the prestressing anchorages of the ring beam and buttresses [17]. The cause was confirmed to be AAR using diagnostic cores. In order to reinstate structural integrity and avoid intrusion of moisture, AECL and ISIS Canada came up with a new remedial program [17]. Concrete that had been deteriorated was eliminated, the ring beam was reinstated, and Glass Fiber Reinforced Polymer (GFRP) wraps were implemented to offer external reinforcement [17]. Fiber optic Bragg grating sensors and strain gauges were installed on the repaired

structure to measure the deformations occurring in it, and the safe life of the safe store was extended at least 50 years [17].

4.3 | Non-Destructive Testing (NDT) and the CONMOD Methodology

Elaborate NDT methods need to be incorporated to inspect gigantic NPP civil structures without interfering with safety [18]. The decommissioned Barsebak Unit 1 reactor containment was used in the European Union project CONMOD (Concrete Containment Modeling and Management) to test and calibrate the advanced NDT methods [18]. Among the key methods considered were Ground-Penetrating Radar (GPR) to map the depth of reinforcement and detect voids, Impact Echo (IE) to detect delaminations and changes in concrete thickness, and Spectral Analysis of Surface Waves (SASW) to measure the velocity of the waves and determine the quality of concrete [18]. The CONMOD methodology has shown that a combination of GPR, IE, and SASW data with sophisticated finite element modeling can form a powerful diagnostic tool, allowing inspectors to identify sub-surface anomalies, measure structural margins, and estimate the remaining service lives.

5 | Analytical and Numerical Modeling of Degraded Reinforced Panels under Multi-Axial Loading

In order to transfer microstructural radiation damage to structural-level design parameters, it is necessary to perform rigorous numerical modeling [9]. Civil members in safety related civil assets, such as reactor walls and biological shields, are mainly reinforced concrete (RC) panels that are exposed to multi-axial in-plane stresses (shear, compression and tension) [9]. The mechanical behavior of nuclear-grade RC panels to different fast neutron fluences has been modeled through analytical investigations using the advanced non-linear finite element program Membrane-2000 which is used to solve panel behavior using the Modified Compression Field Theory (MCFT) [9].

In order to conduct a highly comparative analysis, three levels of progressive degradation (D1, D2 and D3) were modelled in which the experimental fast neutron fluences and corresponding concrete compressive and tensile strength reductions values (calculated in Hilsdorfs compilations) were used [5, 9]. The panels were tested under six multi-axial loading conditions (shear only, shear and biaxial tension, shear and biaxial compression) and a series of reinforcement ratios (0.9% to 3.0%) [9]. Table 3 presents simulated concrete degradation levels and residual engineering properties.

The numerical data set (from Kambayashi et al. [9] and Hilsdorf [5]) shows a leveling off of the residual tensile strength ft at the levels D1, D2 and D3. On the mechanical side, it is a sign of the early stage of the saturation of micro-cracking at the Interfacial Transition Zone (ITZ) between aggregate and mortar, where the initial tensile capacity of the mortar is consumed by the extensive debonding formed during initial fast neutron exposure (D1 = 2.0×10^{19} n/cm^2). Macroscopic tensile degradation does not increase beyond this limit, but compressive strength f'c and elastic modulus Ec decrease monotonically with increasing volumetric aggregate expansion and metamictization.

5.1 | Impact on the Ultimate Shear Capacity

The numerical results show that the structural capacity losses are quite significant and dependent on the reinforcement ratio (ρ) and the loading state [9]. In the case of pure shear and shear-axial loading, the ultimate shear capacity of a highly reinforced panel (ρ > 1.88%) is reduced by 51% under level D3 (2.0×10^{21} n/cm^2) [9]. Ultimate shear strength losses of 11% to 22% due to radiation degradation are found in moderately reinforced elements (ρ = 1.35%) [9]. For shear-biaxial compression, the ultimate capacity is reduced by 29% at level D2 (2.0 × 1020 n/cm2) and by a staggering 62% at level D3, showing that compressive confinement does not stop the panel from collapsing badly at higher fluences [9].

5.2 | Failure Mode Transitions and Ductility Loss

In addition to loss of strength, there is an important shift in failure modes of structure due to radiation degradation [9]. RC Panels are designed to fail in a ductile manner in un-degraded conditions, by yielding of the reinforcing steel. For reinforcement ratios between 0.9% and 1.88%, however, the failure mode of the panels changes from ductile yielding of the steel to sudden brittle crushing of the concrete (crushing of the concrete in the diagonal compression struts) at level D3 radiation [9]. This brittle crushing is the controlling mode of failure even at level D2 for moderately reinforced elements and hence the safety margins of the structures are seriously affected [9].

The decrease in diagonal compressive capacity is controlled by

Table 3 | Simulated concrete degradation levels and residual engineering properties [5, 9].

Degradation Level	Fast Neutron Fluence (n/cm^2)	Residual f'c (%)	Residual ft (%)	Residual Ec (%)	Reference
D1	2.0×10^{19}	95.0% (5% Loss)	49.0% (51% Loss)	90.0% (10% Loss)	[5, 9]
D2	2.0×10^{20}	72.5% (27.5% Loss)	49.0% (51% Loss)	75.0% (25% Loss)	[5, 9]
D3	2.0×10^{21}	40.0% (60% Loss)	49.0% (51% Loss)	45.0% (55% Loss)	[7, 9]

the compression softening effect in cracked concrete, which is modelled in the MCFT as a function of the concurrent principal tensile strain ε_1:

$$f_{c2} = f_{c2\,max} \cdot \left[0.8 + 0.34 \cdot \left(\frac{\varepsilon_1}{\varepsilon_{c'}} \right) \right]^{-1} \quad (4)$$

where f_{c2} is the principal compressive stress, f_{c2max} is the softened compressive strength limit, and $\varepsilon_{c'}$ is the strain at the peak cylinder compressive strength [9]. This relationship is shown in Figure 4, where the aggregate expansion and matrix contraction that result in extensive interfacial tensile cracking directly lead to the loss of diagonal compressive resistance and to premature brittle failure. The plotted relation is mathematical and uses $\varepsilon_{c'} = -0.002$ for illustration.

This failure mode transition is accompanied by a dramatic decrease in structural ductility. With increasing radiation dose, the ductility index (ratio of ultimate deformation to yield deformation) is decreased significantly [9]. The Applied Technology Council guidelines require that all civil structures built to be seismic resistant have an allowable ductility index of less than 3.0. In the D2 and D3 radiation fields, the ductility index of moderately reinforced panels is significantly lower than this regulatory value, and the panels are likely to fail in a catastrophic brittle manner in the event of a seismic or extreme impact [9].

6 | The Paradigm of Structural Health Prognosis and Probabilistic Aging Management

Structural Engineering needs to move from the traditional prescriptive inspection regimes to risk-informed, probabilistic-based aging management programs (AMPs) [1] to ensure global nuclear safety over 80+ years. The most critical civil safety assets, such as the biological shield walls, the basemats and the subterranean foundations, are only partly or not at all accessible, which is why prescriptive visual testing is not sufficient. Advanced AMPs should include continuous SHM and NDE as well as PRA within a continuous Plan-Do-Check-Act (PDCA) framework [4].

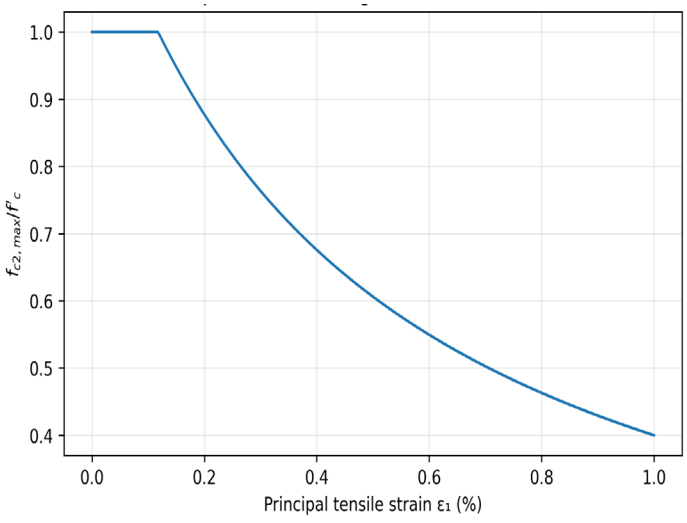


Figure 4 | Compression-softening factor from the Vecchio–Collins MCFT expression.

A full AMP should follow the four-stage cycle below:

• Plan: Make structural classifications and scoping, using Level 1 Seismic PRAs [4]. Probabilistic analyses show that the core damage probability (CDP) can be doubled under seismic loads when structural degradation of concrete shear walls is considered plausible, and that the assets with the highest risk are foundations, basemats and lower biological shield walls.

• Do: Continuous SHM with embedded sensor networks [4]. This includes acoustic emission monitoring, which involves arrays of broadband piezoelectric accelerometers to record acoustic energy generated by microcracks in the structure, and the acoustic energy generated by the breakage of prestressing tendon wires, in real-time, and before catastrophic losses in prestressing are experienced [4, 19].

• Check: Advanced NDT and condition assessments are carried out periodically. Advanced technologies such as Ground-Penetrating Radar, Impact Echo and high-energy industrial radiography (Iridium/Cobalt isotopes or Linac systems) are used to image thick concrete sections, quantify voids and liner debonding, and validate numerical finite-element models [18, 20].

• Act: Implement effective, long-term remedial repairs [17]. Cracks shall be evaluated as dormant or active, with the dormant cracks being injected with low-viscosity epoxy or high molecular weight methacrylate (HMWM) and the active joints being treated as expansion joints [20]. The deteriorated concrete is cut out and replaced with compatible cementitious materials and external Glass Fiber Reinforced Polymer (GFRP) overlays are added to restore monolithic structural integrity [17].

6.1 | Quantitative Probabilistic Reliability Metrics and Limit State Analysis

In order to move towards a true probabilistic AMP, structural performance needs to be assessed using limit state functions g(X) as a function of the vector of stochastic resistance (X) and load variables [1, 4]. The probability of failure Pf is defined as: $Pf = P(g(X) \leq 0) = \int \ldots \int fX(x)\,dx$, where the limit state function is governed by:

$$g(X) = R(t,\phi) - S_E \quad (5)$$

In this case, R(t, Φ) is the time and fluence dependent structural resistance (e.g., shear capacity under MCFT [9]) and SE is the extreme design-basis demand (e.g., seismic acceleration, LOCA pressure) [1, 2]. The reliability index β(t) is given by:

$$\beta(t) = \frac{\mu_g(t)}{\sigma_g(t)} \quad (6)$$

The mean and standard deviation of the limit state safety margin are denoted as μ_g and σ_g, respectively [1, 4]. The safety criteria of USNRC and IAEA require target reliability indices of nuclear containments to be kept at $\beta \geq 3.5$ to 4.2 (annual $P_f < 10^{-5}$ to 10^{-6}) [2, 20]. During the operating time (t), radiation degradation decreases the mean shear capacity and increases the variability (σ_R) of the shear capacity [1, 9]. The results of the NDT inspection (for example, SASW wave velocity or GPR void mapping) can be used to update the prior probability distribution of R(t, Φ) and then make risk-informed decisions on the timing of repairs or operational power derating [4, 18, 20].

7 | Key Knowledge Gaps and Emerging Research Frontiers

Figure 5 proposes a risk-informed aging-management cycle combining PDCA, condition monitoring, mechanistic modeling and reliability assessment. Comprehensive comparative synthesis matrix of concrete degradation mechanisms, modeling approaches and research frontiers are presented in Table 4. Although significant progress has been made in materials science for concrete, there are important missing knowledge areas that are key areas for future research. They are summarized as follows:

• In operating NPPs, concrete structures are not subjected to any one environmental stressor. These advanced computational models should account for the synergistic, coupled effects of the high temperatures, mechanical constraints, moisture migration, and neutron/gamma radiation fields, and simulate the behavior of concrete as a complex, thermodynamic multi-phase system [9].

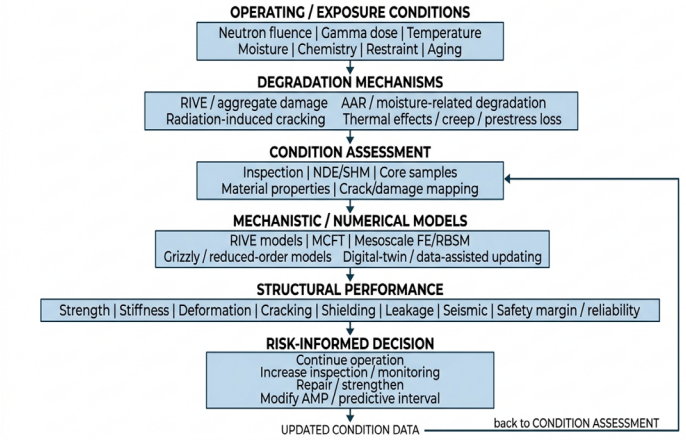


Figure 5 | Proposed risk-informed aging-management cycle combining PDCA, condition monitoring, mechanistic modeling and reliability assessment.

• Characterizing Dose-Rate and Spectrum Effects: Most historical irradiation data have been obtained from test reactors that operate at high flux and high dose rates – not the low flux and long operating times of commercial reactors. Further studies are needed to assess the possible 'rate effects' of radiation induced damage, and to correlate accelerated tests to real-world cores [21].

• The exposure time and aggressive chemical stressors in the

Table 4 | Comprehensive comparative synthesis matrix of concrete degradation mechanisms, modeling approaches and research frontiers [1–22].

Degradation Mechanism / Area	Primary Physical Driver	Current Engineering State / Model	Critical Knowledge Gap / Future Horizon	Reference
Aggregate Expansion (RIVE)	Fast neutron atomic displacements (metamictization)	Empirical exponential kinetics (Eq. 1); quartz sensitivity	Dose-rate spectrum effects; low-flux commercial plant calibration	[3, 7, 8]
Matrix Radiolysis & Drying	Gamma photon energy transfer & water radiolysis	C-S-H dehydration; $Ca(OH)_2$ carbonation & depassivation	Coupled thermodynamics of water migration in thick shielded sections	[10, 11, 13]
Structural Shear Capacity Loss	Synergistic ITZ microcracking & volume mismatch	MCFT non-linear panel simulations (Membrane-2000)	Full-scale 3D multi-axial restraint & boundary condition modeling	[7, 9]
Decommissioning Field Verification	Protracted low-dose operational radiation	Core extraction, petrography, & SEM ettringite analysis	Reconciling laboratory accelerated tests with 60+ year plant cores	[15-17]
Non-Destructive Evaluation (NDE)	Inaccessible civil subelement degradation	GPR, Impact Echo, SASW, & Acoustic Emission (AE)	High-radiation background NDE imaging of thick basemats & liners	[18-20]
Probabilistic AMP & Reliability	Stochastic load & resistance decay over time	PDCA cycle; Limit State g(X) & Reliability Index β(t)	Integration of real-time SHM sensor streams into Bayesian PRA	[1, 2, 4]

concrete around high-level waste (HLW) repositories are different from the ones in a reactor pressure vessel, and so is the radiation field. Limits and durability models need to be specifically determined for structural concrete exposed to radioactive waste streams over centuries [22].

• The need for global NDE of inaccessible, heavily-reinforced civil subelements with the ability to image thick, highly-reinforced structures and basemats under high radiation background levels is critical, in order to detect subsurface and back-side liner corrosion before the structural margins are eroded [4, 18].

8 | Conclusions

Mechanical and structural integrity of safety-related concrete assets is the absolute physical and regulatory cap for LTO and safe-storage decommissioning of nuclear power plants. It is important to reconcile microstructural pathways of radiation damage such as Radiation-Induced Volumetric Expansion (RIVE) and pore-water radiolysis with structural-scale performance loss. The non-linear numerical modeling using Modified Compression Field Theory (MCFT) has shown that under severe levels of radiation field, a catastrophic change of failure mode from highly ductile steel yielding to sudden, brittle crushing of concrete can be triggered and the ultimate shear capacity dropped up to 62% under severe shear-biaxial compression loading conditions for heavily reinforced sections ($\rho > 1.88\%$). These risks can only be mitigated through the use of a combination of the following: use of advanced heavy weight aggregates, use of Supplementary Cementitious Materials (SCMs) and nano-hybrids (1.5 % nano-alumina / 0.1 % carbon nanotubes) and a shift to risk-informed and probabilistic Aging Management Programs (AMPs). Combined use of advanced non-destructive evaluation (NDE) technologies like GPR, Impact Echo, and Acoustic Emission with continuous structural health prognosis will guarantee the security and continued operation of the civil infrastructure of the nuclear fleet worldwide across their multi-decade operational lifetimes.

Reference

1. Naus, D., Oland, C., Ellingwood, B., Graves III, H., and Norris, W., (1996). Aging management of containment structures in nuclear power plants. Nuclear engineering and design, 166(3): 367-379.

2. Commission, U. S. N. R. Generic Aging Lessons Learned (GALL) Report — Final Report (NUREG-1801, Revision 2). 2010 [cited 2026 31.10.2026]; Available from: https://www.nrc.gov/regulations-legislation/nureg-series-publications/publications-prepared-by-nrc-staff/generic-aging-lessons-learned-gall-report-nureg-1801/r2#pubinfo.

3. Kontani, O., Ichikawa, Y., Ishizawa, A., Takizawa, M., and Sato, O., (2014). Irradiation effects on concrete structures. Infrastructure systems for nuclear energy: 459-473.

4. Agarwal, V., Neal, K. D., Mahadevan, S., and Adams, D., Concrete structural health monitoring in nuclear power plants (No. INL/CON-17-41433). 2017, Idaho National Laboratory, Idaho Falls, ID (United States).

5. Hilsdorf, H. K., Kropp, J., and Koch, H. J., (1978). The effects of nuclear radiation on the mechanical properties of concrete. Special Publication, 55: 223-254.

6. Kaplan, M. F., (1989). Concrete radiation shielding : nuclear physics, concrete properties, design and construction. Longman Scientific & Technical.

7. Maruyama, I., Kontani, O., Takizawa, M., Sawada, S., Ishikawao, S., Yasukouchi, J., Sato, O., Etoh, J., and Igari, T., (2017). Development of soundness assessment procedure for concrete members affected by neutron and gamma-ray irradiation. Journal of Advanced Concrete Technology, 15(9): 440-523.

8. Le Pape, Y., Alsaid, M. H., and Giorla, A. B., (2018). Rock-forming minerals radiation-induced volumetric expansion–revisiting literature data. Journal of Advanced Concrete Technology, 16(5): 191-209.

9. Kambayashi, D., Sasano, H., Sawada, S., Suzuki, K., and Maruyama, I., (2020). Numerical analysis of a concrete biological shielding wall under neutron irradiation by 3D RBSM. Journal of Advanced Concrete Technology, 18(10): 618-632.

10. Chilton, A. B., Shultis, J. K., and Faw, R. E., (1984). Principles of radiation shielding. NJ (USA), Prentice Hall Inc.

11. Maruyama, I., Ishikawa, S., Yasukouchi, J., Sawada, S., Kurihara, R., Takizawa, M., and Kontani, O., (2018). Impact of gamma-ray irradiation on hardened white Portland cement pastes exposed to atmosphere. Cement and Concrete Research, 108: 59-71.

12. Masoud, M. A., Kansouh, W., Shahien, M., Sakr, K., Rashad, A. M., and Zayed, A., (2020). An experimental investigation on the effects of barite/hematite on the radiation shielding properties of serpentine concretes. Progress in Nuclear Energy, 120: 103220.

13. Rasheed, P. A., Nayar, S. K., Barsoum, I., and Alfantazi, A., (2022). Degradation of concrete structures in nuclear power plants: A review of the major causes and possible preventive measures. Energies, 15(21): 8011.

14. El-Sayed, A. A., Fathy, I. N., Tayeh, B. A., and Almeshal, I., (2022). Using artificial neural networks for predicting mechanical and radiation shielding properties of different nano-concretes exposed to elevated temperature. Construction and Building Materials, 324: 126663.

15. Konno, T. Concrete Properties Influenced by Radiation Dose During Reactor Operation. in Proceedings of the OECD-NEA workshop on the evaluation of defects, repair criteria and methods of repair for concrete structures on nuclear power plants. 2002. 262-271.

16. Chenier, J.-O., Komljenovic, D., Gocevski, V., Picard, S., and Chrétien, G., (2012). An approach regarding aging management program for concrete containment structure at the gentilly-2 nuclear power plant. Proceedings of the Canadian Nuclear Society.

17. Popovic, A., Panesar, D., and Elgohary, M. Repair of the Gentilly-1 concrete containment structure. in Proceedings of the OECD-NEA workshop on the evaluation of defects, repair criteria and methods of repair for concrete structures on nuclear power plants. 2002. 39-50.

18. Jovall, O., Larsson, J.-A., Shaw, P., Touret, J.-P., and Karlberg, G. Concrete containment modeling and management, Conmod. in Proceedings of the 17th international conference on structural mechanics in reactor technology. 2003. 1607-1614.

19. Simon, A. and Courtois, A., (2011). Structural monitoring of prestressed concrete containments of nuclear power plants for ageing management. Structural Mechanics in Reactor Technology, 21: 6-11.

20. Clifton, J., (1991). Predicting the remaining service life of concrete, NISTIR 4712. Institute of Standards and Technology.

21. Remec, I., Rosseel, T. M., Field, K. G., and Pape, Y. L. Characterization of radiation fields for assessing concrete degradation in biological shields of NPPs. in EPJ Web of Conferences. 2017. EDP Sciences 05009.

22. Attar, A., Gencturk, B., Hanifehzadeh, M., and Willam, K., (2016). Accelerated aging of concrete dry cask storage systems for nuclear waste. Journal of Advanced Concrete Technology, 14(6): 299-310.

Acknowledgements

-

Funding

This research did not receive any specific grant from funding agencies in the public, commercial, or not-for-profit sectors.

Ethics Statement

It does not contain any experimental studies involving human participants or animal subjects performed by any of the authors.

Conflicts of Interest

The authors declare no conflicts of interest.

Authors Contribution

The first author and second author have equal contribution in the research work. All authors read and approved the final manuscript.

Data Availability Statement

The data that support the findings of this study are available on request from the corresponding author.